High resolution rotational and v3 coherent Raman spectra of C2H6

Abdullah AlKahtani, Salvador Montero, and Joseph W. Nibler

Citation: The Journal of Chemical Physics **98**, 101 (1993); doi: 10.1063/1.464658
View online: http://dx.doi.org/10.1063/1.464658
View Table of Contents: http://scitation.aip.org/content/aip/journal/jcp/98/1?ver=pdfcov
Published by the AIP Publishing

High resolution rotational and ν_3 coherent Raman spectra of C_2H_6

Abdullah Al-Kahtani, Salvador Montero,[a] and Joseph W. Nibler[b]
Department of Chemistry, Oregon State University, Corvallis, Oregon 97331

(Received 11 August 1992; accepted 23 September 1992)

Coherent anti-Stokes Raman spectroscopy has been used to study C_2H_6 in the rotational and ν_3 CC stretching regions. Pure rotational transitions for torsionally excited molecules are seen for the first time and direct analysis of the peak maxima gives B values of 0.663 06 and 0.660 37 cm^{-1} for the $v_4=0$ and 1 torsional levels. The change in B is combined with *ab initio* calculations to show that the primary response of the molecule to the increased torsional amplitude is a CC extension of 0.0031 Å, plus a slight increase of 0.10 degrees in the CCH angle. For the ν_3 vibrational Q branch, a complex mixture of four band systems is seen, a consequence of Fermi resonance interactions causing the predicted four torsional sublevels of this state to separate. Spectra of jet-cooled samples aid in the assignment of the spectrum and the four torsional components are determined as 994.973 (E_{3s}), 994.878 (E_{3d}), 994.864 (A_{1s}), and 993.791 cm^{-1} (A_{3d}). The A and B rotational constants decrease by 0.003 27 and 0.006 21 cm^{-1}, respectively, when ethane is excited in the ν_3 mode. These differences are used with the *ab initio* results to deduce that this transition results in a net increase of 0.010 Å in the average CC distance, accompanied by a decrease of 0.12 degrees in the CCH angle and a very small CH decrease of 0.0002 Å. The calculations also suggest that the V_3 torsional barrier for the $v_3=1$ state is about 3% smaller than for the ground state.

I. INTRODUCTION

Since it serves as the prototype for molecules with internal torsional motion, ethane has drawn the attention of experimentalists and theoreticians for many years.[1] Most of the interest has centered on the determination of the form and height of the potential barrier experienced as the CH_3 groups counter-rotate, information most directly extracted from transitions and splittings measured for the lowest torsional levels. The fundamental torsional transition (ν_4) is formally infrared and Raman inactive, however, some weak dipole intensity has been seen in the infrared due to Coriolis interactions with other modes.[2] Recently, Ozier and co-workers have obtained high resolution infrared spectra of the $1\leftarrow0$ transition centered near 285 cm^{-1} and analyses of tunneling splittings in this and the $2\leftarrow1$ hot band showed that the torsional potential is well described by cosine terms with $V_3=1011.89$ cm^{-1} and $V_6=10.768$ cm^{-1}.[3]

Similar potential parameters have been deduced from lower resolution Raman spectra of $v_4=2\leftarrow0$, $3\leftarrow1$, $4\leftarrow2$, and $5\leftarrow3$ transitions.[4,5] Raman studies have also given some pure rotational data.[6,7] In this paper, we report improved rotational Raman data, obtained at higher resolution using coherent anti-Stokes Raman spectroscopy (CARS). A number of new hot band features are seen in the pure rotational region and the analysis of these is presented. The resulting rotational constants are then combined with *ab initio* calculations to deduce specific structural changes that occur as the torsional excitation increases.

We have also examined the ν_3 CC stretching mode region using high resolution CARS spectroscopy. A complex Q-branch pattern is observed, whose analysis is greatly aided by obtaining CARS spectra of samples cooled in a supersonic expansion. This ν_3 transition is especially interesting since all four predicted torsional sublevels of the upper state are observed. These sublevels are a consequence of the fact that ethane contains two CH_3 rotors, yielding six states for all vibrational levels. Each totally symmetric (A_{1s}) vibrational state is predicted to yield sublevels of A_{1s}, A_{3d}, E_{1s}, and E_{3d} symmetry in the appropriate G_{36}^{+} double group representation.[8] The spacings between these sublevels are very small in the $\nu_4=0$ state and have not been measured. However, these increase rapidly for higher torsional states and for $4\nu_4$, near the top of the barrier, the sublevels extend over 150 cm^{-1}.

Little is known about the magnitude of the splittings for excited states of modes not involving torsion, although values less than 0.05 cm^{-1} have been measured for the upper state of the infrared active ν_9 CH_3 rocking mode.[9] Similar spacings might be anticipated for the Raman active ν_3 mode but, in fact, much larger values are indicated by our CARS spectra, a consequence we believe of Fermi resonance interactions between ν_3 and the $n\nu_4$ levels. An analysis of the CARS spectrum is presented in this paper, along with some discussion of the CH bond length and CCH bond angle changes that accompany the CC excitation. We note also that an independent study of the ν_3 region has been made using a high resolution stimulated Raman spectrometer in Madrid and a more detailed discussion of the analysis of this band and of the interaction between the CC stretch and the torsional mode will be published separately.[10]

[a]Permanent address: Instituto de Estructura de la Materia, C.S.I.C. Serrano 123, Madrid 28006, Spain.
[b]Author to whom correspondence should be addressed.

II. EXPERIMENTAL

The high resolution CARS apparatus utilized for most of this study was modified recently in order to be used in both vibrational and pure rotational regions with minimal change in the optical arrangement.[11] Briefly, the system uses a seeded, single frequency Nd-YAG laser which is doubled to give 8 ns 532 nm pulses at 10 Hz. Part of the green light is used to pump an amplifier chain for a tunable ring dye laser and this is then mixed with two fractions of 532 nm light focused into the sample in a noncollinear (folded BOXCARS) phase matching arrangement. The resultant CARS signal is spatially filtered, collimated, and directed through a monochromator to a photomultiplier whose output is averaged and digitized for computer analysis.

The Nd-YAG pump frequency was determined by the cw seed laser whose output was temperature tuned so that the frequency matched the absorption of a known I_2 line in a cell. The Stokes dye laser output was also calibrated with a 10 cm I_2 absorption cell and the Raman frequencies were obtained from the pump and dye frequency difference. The effective instrumental resolution was about 0.005 cm^{-1} and the absolute frequency accuracy is estimated to be ± 0.01 cm^{-1}, although the relative frequencies are believed to be somewhat better.

For the pure rotational Raman studies, one of the 532 nm input beams was replaced by light at 568.2 nm from a single-mode coherent Kr^+ ion laser whose output was directed through a second three-stage amplifier chain. The amplified ring dye output was tuned to operate in the range overlapping this yellow Kr^+ line so as to drive the rotational transitions coherently. The 532 nm source was then used as a probe to generate the anti-Stokes signal photons at a slightly shorter wavelength and with orthogonal polarization. In this way, it was possible to scan to zero Raman shift using optical filters to eliminate scattered yellow light and a polarizer to reject 532 nm photons.

The ethane (Matheson 99.0%) was used directly from the cylinder and placed in a 20 cm cell for the static sample measurements at room temperature. In some experiments on the ν_3 band, jet spectra were obtained for pure or helium mixtures using a pulsed valve assembly with a shim nozzle of 0.250 mm diameter.

III. RESULTS

A. Pure rotational spectra

The pure rotational CARS spectra of C_2H_6 were measured using static samples at room temperature and at pressures of 50 to 200 Torr. The signals were relatively weak for the single-pass noncollinear imaging used but nonetheless, $S(J)$ lines from $J=10$ to 30 were directly measured for the ground state. Because of the low value of I_A/I_B (~ 0.25) it is expected that the S branch will be much more intense than the $\Delta J=\pm 1R$ branch,[12] which is allowed but was not observed. Figure 1 shows CARS spectra of representative $S(15)$ and $S(25)$ lines. No indication was seen of K structure caused by centrifugal distortion and, indeed, such would not be expected from the small

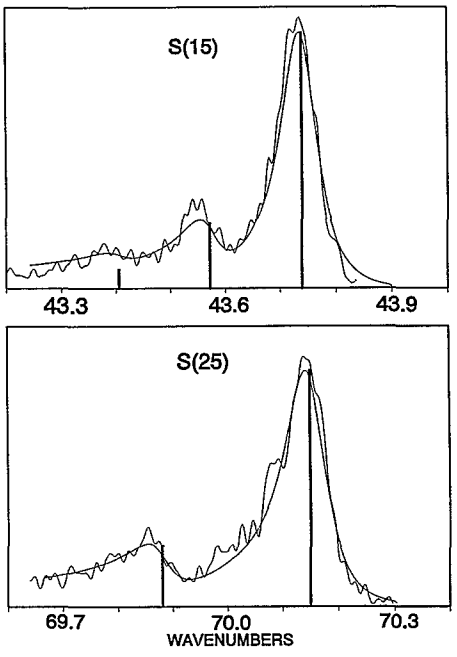

FIG. 1. Observed and simulated CARS spectra for $S(15)$ and $S(25)$ rotational lines of C_2H_6. Simulations are based on the corrected "stick" transitions as described in the text.

magnitude of D_{JK} deduced in infrared studies.[13] Likewise, structure due to the tunneling sublevels would not be expected to be resolvable. However, one and in some cases two shoulders were resolved for each S line and these are attributed to rotational transitions originating from molecules in the $\upsilon_4=1$ and 2 torsional states.

A tabulation of the peak maxima for the $\upsilon_4=0$ and 1 rotational transitions is given in Table I. For a symmetric top, these rotational S branch frequencies are given by

$$S(J,K)=(4B-6D_J-4D_{JK}K^2)(J+\tfrac{3}{2})-8D_J(J+\tfrac{3}{2})^3. \quad (1)$$

Since no K structure was resolved, the D_{JK} term was taken to be zero in a least squares analysis of these peak frequencies to extract the rotational parameters shown in Table II. These values are about an order of magnitude more precise than data from earlier Raman studies.[6,7] In the latter, the resolution did not permit distinction of the hot band sequences, hence the B value deduced is intermediate between our $\upsilon_4=0$ and 1 results.

Our rotational parameters are also in good agreement with the more accurate values from infrared vibrational–rotational data,[13,14] although B for the hot band is lower by slightly more than the estimated uncertainties. The measured hot band features are also slightly lower (0.009 cm^{-1} average) than the $K=3$ maxima calculated from the infrared constants. We note that, if these maxima are fit with D_{JK} omitted, the decrease in the infrared B value is only 2.5×10^{-5} cm^{-1}, too small to attribute the discrepancy to fitting model. It is possible that it can arise from the fact that the CARS peak frequencies may differ slightly from the true transition frequencies due to small shifts in the

TABLE I. S-branch rotational transitions (cm^{-1}) for C_2H_6.

	$v_4=0$			$v_4=1$		
J	ν_{Peak}	$\nu_{Corr.}$[a]	ν_{ir}[b]	ν_{Peak}	$\nu_{Corr.}$[a]	ν_{ir}[b]
10	30.476	30.485	30.486	...	...	...
11	33.137	33.145	33.134	33.004	33.019	33.008
12	35.785	35.791	35.782	35.639	35.655	35.645
13	38.437	38.442	38.429	38.282	38.299	38.282
14	41.080	41.085	41.075	40.918	40.935	40.919
15	43.722	43.727	43.721	43.542	43.560	43.554
16	46.368	46.373	46.366	46.180	46.199	46.189
17	49.013	49.018	49.010	48.817	48.836	48.823
18	51.648	51.653	51.653	51.447	51.466	51.456
19	54.294	54.299	54.295	54.080	54.098	54.088
20	56.931	56.936	56.936	56.706	56.727	56.719
21	59.580	59.586	59.576	59.341	59.362	59.350
22	62.218	62.224	62.215	61.973	61.995	61.978
23	64.856	64.862	64.853	...	...	...
24	67.487	67.494	67.489	67.227	67.250	67.233
25	70.127	70.134	70.125	69.843	69.866	69.858
26	72.754	72.763	72.759	72.471	72.495	72.482
27	75.385	75.395	75.391	75.093	75.119	75.105
28	78.016	78.026	78.022	77.712	77.737	77.726
29	80.647	80.660	80.652	80.329	80.356	80.346
30	83.271	83.285	83.280	82.957	82.985	82.964

[a]See the text for discussion of corrections due to CARS interference effects.
[b]Values of ν_{ir} are calculated for the most intense $K=3$ transitions using the constants referenced in Table II.

maxima caused by CARS interference effects between adjacent peaks and by nonresonant contributions to the third order susceptibility. Such effects are discussed in Ref. 11 and an effort to obtain corrected transition values from spectral simulations is described below.

B. Simulation of rotational spectra

The imaginary part of the third order susceptibility χ'' is the key element in calculating the CARS intensity of an $S(J,K)$ line and its peak relative value at resonance is

$$\chi''_{JK}(\text{CARS}) = g_{JK} b_{JK,J+2K} [e^{-F_{JK}/kT} - e^{-F_{J+2K}/kT}]. \quad (2)$$

TABLE II. Rotational constants (cm^{-1}) for C_2H_6.

$v_4=0$	B	$D_J\times10^6$	$D_{JK}\times10^6$
From ν_{Peak}[a]	0.663 06(6)	1.09(4)	...
From $\nu_{Corr.}$[a]	0.663 13(6)	1.08(4)	...
Raman[b]	0.662 1(5)	0.94	...
Raman[c]	0.662 7(4)	1.06	...
Infrared[d]	0.663 028(2)	1.032(2)	2.65(9)
$v_4=1$			
From ν_{Peak}	0.660 37(5)	1.020(3)	...
From $\nu_{Corr.}$	0.660 66(6)	1.06(4)	...
Infrared[e]	0.660 497(9)	1.020(5)	2.72(2)

[a]Uncertainties are twice the standard errors.
[b]Reference 6.
[c]Reference 7.
[d]Reference 13.
[e]Averages over four torsional sublevels given in Ref. 14. The standard deviation of these averages are given in parentheses.

Here $F(J,K)$ is the usual energy level term value and $b_{JK,J+2K}$ is given by[12]

$$b_{JK,J+2K} = \frac{3[(J+1)^2-K^2][(J+2)^2-K^2]}{2(J+1)(J+2)(2J+1)(2J+3)}, \quad (3)$$

while the degeneracy $g_{JK}=2g_{ns}(2J+1)$. The nuclear spin statistical weight g_{ns} for unresolved tunneling substates is 8 ($K=0$, J even), 16 ($K=0$, J odd), 24 ($K=3,6,9,\cdots$), or 20 ($K=1,2,4,5,\cdots$). Since the K structure is very small and was not resolved in our spectra, we have summed over K in obtaining a single χ'' for each J line. For the $v_4=1$ and 2 lines, the peak susceptibilities are reduced by the appropriate vibrational Boltzmann factors.

To generate a spectrum from the peak values, the various line broadening contributions must be considered. The Gaussian Doppler width was calculated taking the crossed beam geometry into consideration and was quite small, of the order of 0.001 cm^{-1}. The instrumental resolution, also assumed Gaussian, was taken to be 0.01 cm^{-1} to include likely broadening due to the AC Stark effect (which is larger for rotational than for vibrational transitions). The main broadening is attributed to collisions since most of the measurements were made at ~200 Torr. From the simulation process, a Lorentzian width $\Delta\nu_{COL}$ of 0.08 cm^{-1} gave the best overall fit of the spectral features.

Since lines of different J are widely spaced, each $S(J)$ pattern was fit independently. In simulating the CARS pattern, it was necessary to add a real nonresonant contribution χ_{NR} to the collision-broadened Lorentzian and a summation was done over the $v_4=0$, 1 and 2 components. A Gaussian function was then convoluted over both the real and imaginary parts of the Lorentzian line shapes to account for the Doppler effect. Finally, the real and imaginary parts of χ were squared, added, and convoluted by the Gaussian laser line shape function using a Fourier transform method. A single value of χ_{NR} was chosen which reproduced the shapes of most features and line width values were also held constant for all $S(J)$ lines.

For each $S(J)$ region, the experimental peak maxima served as the initial choice of the true resonances. The difference between these and the maxima of the convoluted spectrum was then applied to get improved resonance values and the process was repeated several times until the convoluted and experimental curves gave good visual agreement. The quality of the fit for the $S(15)$ and $S(25)$ regions can be seen in Fig. 1. The shift between the corrected frequency (stick) and the convoluted maximum is apparent and is about three times as large for the weaker hot band features as for the ground state, as expected.

The frequencies resulting from these corrections are shown in Table I and the rotational parameters that they produce are given in Table II. As can be seen, the main effect was to raise B for both states so that these values now lie slightly *above* the infrared values. In general, the ground state frequencies were raised about 0.007 cm^{-1}, while the hot band values increased by 0.021 cm^{-1}, making *both* sets an average 0.009 cm^{-1} higher than the infrared transitions. This may be indicative of a systematic frequency error in our measurements although we note that this discrepancy

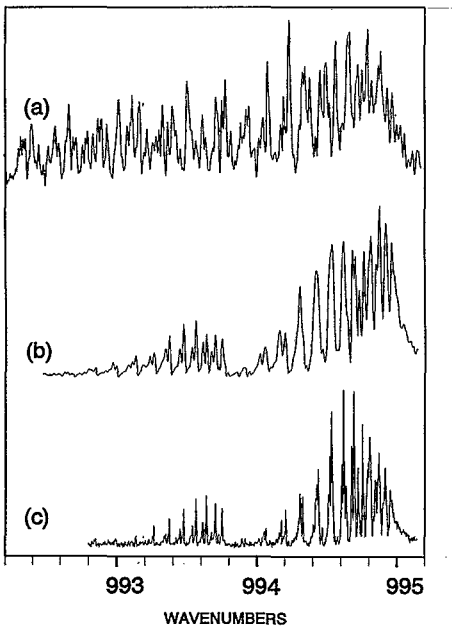

FIG. 2. CARS Q-branch spectra of C_2H_6 in the ν_3 region. (a) 34 Torr C_2H_6 in a static cell at room temperature. (b) Neat C_2H_6 in a 2.4 atm free jet expansion at $X/D=7$. (c) 50% C_2H_6 in He in a 4.4 atm free jet expansion at $X/D=6$.

is within our estimated frequency uncertainty of 0.01 cm^{-1}. It seems clear that to improve frequency measurements of this type significantly, more experimental effort should be made to improve our calibrations and to reduce line widths by using lower sample pressures and laser powers. We estimate that this, combined with careful simulations of the type described here, could probably improve the accuracy of the frequencies and parameters an order of magnitude.

C. CARS spectra of the ν_3 region of C_2H_6

The ν_3 region (900–1100 cm^{-1}) has been the subject of two Raman studies in the past. In the first, a ν_3 band origin of 994.8 cm^{-1} was obtained by analyzing the resolved O and S branches accompanying the strong Q branch.[7] More recently, Helvoort *et al.* measured the Q-branch position in both static cell and free jet expansion experiments and, from simulations, deduced a somewhat different value of 992.9 cm^{-1}.[4] The Q branch was not resolved in either experiment nor were any hot bands involving the torsion (ν_4) distinguished.

In the present work, the high resolution CARS spectrum of a room temperature sample at 34 Torr reveals an exceptionally dense, irregular pattern in the Q-branch region from 990–1000 cm^{-1} [Fig. 2(a)]. Such complexity could arise from contributions by torsional hot bands or by torsional splittings, although as mentioned earlier the latter were expected to be small. To simplify the spectrum, jet spectra were taken for pure samples and for 50% mixtures in helium [Figs. 2(b) and 2(c)]. It is clear that cooling of ethane in the jet resulted in a more tractable spectrum, with two different band progressions apparently revealed. The jet spectra thus serve as the basis for the analysis discussed below. It should be noted that the three spectra shown are representative of several scans that were taken of both pure and seeded C_2H_6 and that the frequencies used in the analysis were obtained as averages of two to five measurements.

D. Spectral analysis of ν_3

1. Possible role of hot bands

The weaker low frequency band sequence is fairly clean and we initially considered the possibility that it corresponded to the torsional hot band. That such a vibrationally hot band could be seen in the jet is not impossible since it is known that vibrational cooling can be less effective than rotational cooling in free jet expansions. However, the band intensity relative to the higher frequency band sequence seemed too high to be consistent with the initial thermal population of the torsion. In addition, consideration of all other hot bands for C_2H_6 shows that they would occur well above the 1000 cm^{-1} region and would have even lower intensity. Finally, attempts to analyze the spectrum as a simple symmetric top Q branch gave unreasonable rotational parameters and poor simulations of the variation of the spectrum with temperature.

Supporting evidence that torsional hot bands need not be considered in the jet spectra comes from the ethane studies of Helvoort *et al.*[4] Although their resolution was insufficient to see the ν_3 structure of interest, they did study other bands where torsional hot bands were observed to disappear on cooling in a jet. A similar observation was made by Owyoung *et al.*[15] in a jet study of the complex ν_1 region of C_2H_6. Thus efficient collisional depopulation of the higher torsional levels seems to occur readily in ethane expansions.

2. Possible role of torsional sublevels

The elimination of hot band contributions leaves then the probability that the extra Q bands in the ν_3 region are due to torsional splittings in the upper state. However, the 1 cm^{-1} separation of the two sequences seems much too large to be consistent with the very small splittings (<0.05 cm^{-1}) seen for the nearby ν_9 mode at 822 cm^{-1}.[9] Instead it seems clear that the four nearly degenerate tunneling sublevels are perturbed by the four widely separated levels of the $v=4$ levels of the torsional mode, a possibility suggested by Helvoort *et al.*[4] but not previously demonstrated.

Figure 3 shows the pattern of likely Fermi resonant interactions between states of the same symmetry in the G_{36}^{+} representation. The $4\nu_4$ levels are calculated values from Ref. 5 and are very close to similar ones given in Ref. 4. From the relative $4\nu_4$ level ordering, one would expect the A_{3d} torsional sublevel of ν_3 to have a relatively large shift to *lower* frequency. The other three sublevels will have smaller shifts to *higher* frequencies, yielding the likely ordering $E_{3s} > E_{3d} > A_{1s} > \nu_3$ origin $> A_{3d}$. Additional shifts

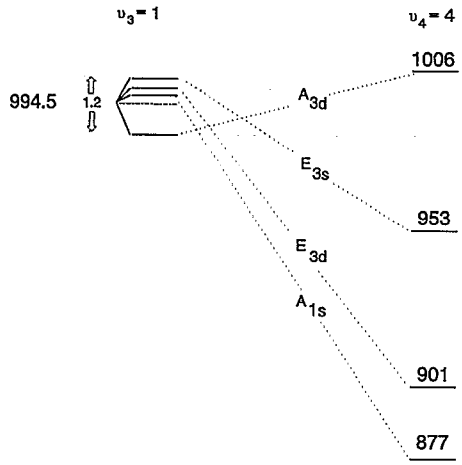

FIG. 3. Energy levels distribution and possible Fermi resonance interaction in the ν_3 region of C_2H_6.

by other $n\nu_4$ levels will occur, but this ordering is consistent with the rotational analysis of the observed spectrum discussed below.

3. Statistical weights

To analyze the spectrum, it is necessary to know the symmetries and statistical weights of each J,K level, as described by Hougen.[8] The net vibration–rotation–torsion symmetry species can be formed as the direct product of the vibration, rotation, and torsion species. For totally symmetric states such as ν_3 and $4\nu_4$ the vibrational symmetry species is A_{1s} and the torsional sublevels are A_{1s}, E_{3s}, A_{3d}, and E_{3d}. The species of the rotational functions depend only on the quantum number K and exhibit a periodicity of 6; for $K=1$, 2, 3, 4, 5, and 6 the species are E_{2d}, E_{1s}, $A_{3d}+A_{4d}$, E_{1s}, E_{2d}, and $A_{1s}+A_{2s}$, respectively. For $K=0$ the species are A_{1s} for J even and A_{2s} for J odd. The nuclear spin species of the six protons are $10A_{1s}+6A_{4s}+3E_{1s}+E_{2s}+3E_{3s}+E_{4s}+8G$ and the total overall symmetry must be A_{2s} or A_{4s} to yield a sign change on exchange of any two protons. Table III gives the nuclear spin species for each allowed level and it can be seen that the A_{1s} and E_{3s} torsional sublevels have rotational states of even K only while the A_{3d} and E_{3d} torsional sublevels have odd K only. Note that the weighting coefficients of the nuclear spin species can be added to give the total nuclear spin statistical weight for each sublevel.

TABLE III. Nuclear spin species and statistical weights for the four torsional sublevels of the A_{1s} vibrational levels of C_2H_6.

	A_{1s}	E_{3s}	A_{3d}	E_{3d}
J even $K=0$	$6A_{4s}$	$2E_{4s}$	···	···
J odd	$10A_{1s}$	$6E_{3s}$	···	···
$K=1,5,7,\cdots$	···	···	$3E_{1s}+E_{2s}$	$16G_s$
$K=2,4,8,\cdots$	$3E_{1s}+E_{2s}$	$16G_s$	···	···
$K=3,9,15,\cdots$	···	···	$10A_{1s}+6A_{4s}$	$6E_{3s}+2E_{4s}$
$K=6,12,18,\cdots$	$10A_{1s}+6A_{4s}$	$6E_{3s}+2E_{4s}$	···	···

4. Assignments

Ethane is a prolate symmetric top and for the parallel ν_3 transition, the Raman active Q-branch ($\Delta J=0$, $\Delta K=0$) transitions will occur at

$$Q(J,K)=\nu_3+(B'-B'')J(J+1)+[(A'-B')-(A''-B'')]K^2-(D'_J-D''_J)J^2(J+1)^2-(D'_{JK}-D''_{JK})J(J+1)K^2-(D'_K-D''_K)K^4. \quad (4)$$

The analysis to extract ν_3 and the rotational parameter differences was first done for the low frequency band using trace(c) of Fig. 2. This band was assigned as the A_{3d} torsional subband of ν_3 for which one expects only transitions from odd K levels with statistical weights of 4 for $K=1$, 5, 7, $\cdots$ and 16 for $K=3$, 9, 15, $\cdots$. At the low temperatures in the jet, therefore, one would expect a simple progression in J with some K structure corresponding mainly to $K=1$ and 3, with $K=3$ more intense because of the higher statistical weight. This assignment is supported by the sudden drop in the intensity at the band head region since the first strong line in the band would be $J=3$, $K=3$ which has much higher intensity than $J=1$, 2, or 3 in the $K=1$ sequence.

In the analysis, an initial assignment of the strong lines in the A_{3d} band region was made and these transitions were fit by linear regression to Eq. (4). The resulting constants were used to calculate other transitions and then weaker lines were added to the least squares set and the process was repeated until most of the lines in the A_{3d} band region were accounted for. Table IV gives the measured frequencies for the A_{3d} transitions, obtained as averages of three different experimental measurements. Those marked with (a) were used in the fit. The assignments and a simulated spectrum, which will be discussed later, are shown in Fig. 4.

In analyzing the three overlapping high frequency Q bands, the assumption was made that the rotational parameters were the same for all four torsional sublevels. Only different ν_3 values were chosen for the three higher Q branches and these were varied until a clear assignment of many of the isolated lines was established. These were then used with the A_{3d} data in a simultaneous fit of all four sublevels. Some of the weaker features were then assigned and the process was repeated until finally all the transitions indicated with an (a) in Tables IV and V were used in obtaining the parameters shown in Table VI. In general, the small magnitude of the obs.—calc. differences shown in Tables IV and V can be taken as good support for the correctness of the assignments. It should be noted that the centrifugal distortion difference parameters were not included in the final fit because they were not well determined due to the low J,K range of the transitions seen in the jet spectra.

TABLE IV. Q-branch transitions (cm^{-1}) of A_{3d} and E_{3d} components of ν_3 for C_2H_6.

		A_{3d}		E_{3d}	
J	K	Obs.	Obs.—Calc	Obs.	Obs.—Calc
1	1	993.793	0.012	994.870	0.002
2	1	993.766	0.010	994.845[a]	0.001
3	3	993.747[a]	0.004	994.827	−0.002
3	1	993.720[a]	0.001	994.804[a]	−0.002
4	3	993.697[a]	0.004	994.778	−0.001
4	1	993.670[a]	0.000	994.755[a]	−0.002
5	3	993.635[a]	0.004	994.719[a]	0.001
5	1	993.608[a]	0.000	994.693	−0.001
6	3	993.560[a]	0.003	994.643	0.000
6	1	993.533[a]	0.000	994.618[a]	−0.001
7	7	993.584[a]	−0.003	···	···
7	5	993.516[a]	−0.001	···	···
7	3	993.473[a]	0.003	994.556	0.000
7	1	993.446[a]	0.000	994.534[a]	0.001
8	5	993.419[a]	0.002	···	···
8	3	993.372[a]	0.001	994.456	−0.001
8	1	993.342[a]	−0.005	994.433[a]	0.000
9	3	993.260[a]	0.002	994.344	−0.001
9	1	993.233[a]	−0.002	994.323[a]	0.001
10	5	993.181[a]	0.000	···	···
10	3	993.133[a]	−0.002	994.224	0.003
10	1	993.105[a]	−0.005	994.199[a]	0.002
11	3	992.993[a]	−0.005	994.087	0.003
11	1	992.971[a]	−0.003	994.062[a]	0.002
12	3	992.850[a]	0.001	···	···
12	1	992.816	−0.009	···	···

[a]Data used in obtaining parameters of Table VI.

TABLE V. Q-branch transitions (cm^{-1}) of A_{1s} and E_{3s} components of ν_3 for C_2H_6.

		A_{1s}		E_{3s}	
J	K	Obs.	Obs.—Calc	Obs.	Obs.—Calc
0	0	994.864	−0.001	994.974	0.000
1	0	994.856	0.004	994.960	−0.001
2	2	994.840	0.000	994.948[a]	0.001
2	0	994.826	−0.002	994.933	−0.003
3	2	994.802	0.000	994.910[a]	0.000
3	0	994.788	−0.002	994.902	0.003
4	4	···	···	994.895	−0.001
4	2	994.753	0.000	994.857	−0.003
4	0	994.739	−0.001	994.846	−0.003
5	4	···	···	994.840	0.006
5	2	994.692	0.002	994.803	0.004
5	0	994.678[a]	0.000	994.788	0.001
6	4	···	···	994.763	0.004
6	2	994.616	0.001	994.725[a]	0.001
6	0	994.603[a]	−0.001	994.717	0.004
7	4	···	···	994.676	0.003
7	2	994.527	−0.001	994.636[a]	−0.001
7	0	994.517[a]	0.000	994.624	−0.001
8	4	···	···	994.577	0.004
8	2	994.429	0.000	994.536	−0.001
8	0	994.418	0.000	994.527	0.001
9	4	···	···	994.464	0.003
9	2	994.318	0.001	994.425[a]	−0.001
9	0	994.305	−0.001	994.415	0.001
10	4	···	···	994.339	0.002
10	2	994.192	−0.001	994.303	0.001
10	0	994.183	0.002	994.291	0.001
11	4	···	···	994.202	0.002
11	2	994.056	0.000	994.165	−0.001
11	0	994.049	0.004	994.153	0.000
12	2	993.906	−0.001	994.016	0.000
12	0	993.896	0.000	994.004	0.000

[a]Data used in obtaining parameters of Table VI.

5. Spectral simulation

A key part of the spectral analysis was the generation of simulated spectra based on the predictions of Fermi resonance and the statistical weights. The simulation process was similar to that in the rotational region but differed in that the anisotropic intensity factor $b_{J,K}$ was neglected. This is reasonable since the Q-branch scattering is mainly isotropic so that the intensity is determined by the statistical weights and Boltzmann factors.[12] Interestingly, from Table II it can be seen that at 0 K C_2H_6 population collapses to three rotational levels ($K=0$, $J=0,1$; $K=1$, $J=1$), with unique nuclear spin sets which are presumed not to interconvert on the time scale of the expansion. Accordingly, separate partition functions were calculated for each spin form, although at the relatively high rotational temperatures reached in these jet experiments this refinement proved minor. The instrumental line width was determined to be 0.005 cm^{-1} from calibrations with a CO_2 jet and, by empirical adjustment, a collisional line width of about 0.003 cm^{-1} was found to reproduce the observed spectrum. A Doppler line width of 0.0009 cm^{-1} was calculated using a jet temperature of 50 K, a value estimated for the rotational temperature from simulations of the A_{3d} region shown in Fig 4.

For the other three sublevels the assignment and simulated spectra are shown in Fig. 5. Displayed below are the simulations of each component to make clearer the J,K assignments. At the top, all three components were included in the simulation and the result compares favorably with the experimental trace. A similar fitting of the room temperature spectrum was done which was in fair accord with the observed spectrum but with some anomalies in positions and intensities. These could be due to hot band contributions or to parameter errors resulting from the limited J,K data range of the jet spectra. Since a detailed analysis of the stimulated Raman data of warmer static

TABLE VI. Vibrational–rotational parameters (cm^{-1}) for ν_3 mode of C_2H_6.

ν_3(CARS)[a]	E_{3s}	994.973(5)[a]	$A''-A'$	0.003 27(9)
	E_{3d}	994.878(5)	A'	2.667 27(9)
	A_{1s}	994.864(5)	$B''-B'$	0.006 21(2)
	A_{3d}	993.791(5)	B'(CARS)	0.656 82(2)[c]
ν_3(Raman)		994.8[d]	B'(Raman)	0.6551[d]
		992.9[e]		

[a]Uncertainties are twice the standard errors.
[b]Using $A''=2.670\ 54\ cm^{-1}$ from Ref. 3.
[c]Using $B''=0.663\ 028\ cm^{-1}$ from Ref. 13.
[d]Reference 7.
[e]Reference 4.

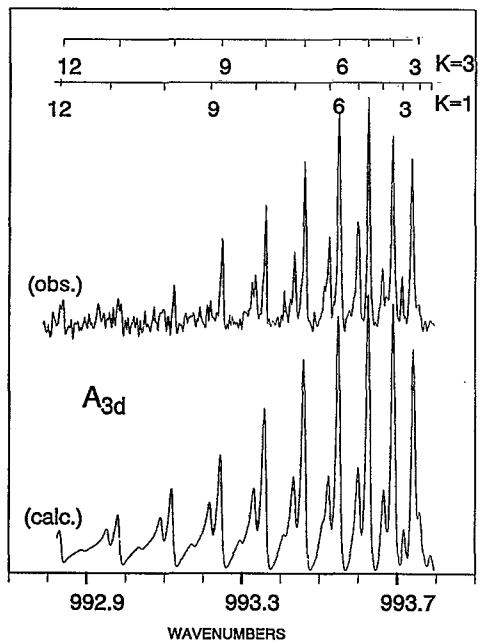

FIG. 4. Observed and simulated Q-branch spectra of A_{3d} torsional component of ν_3 for C_2H_6 at 50 K.

samples was underway in Madrid, a more concentrated effort on the CARS data was not undertaken.

IV. DISCUSSION

A. Effect of torsional excitation

It is interesting to consider the structural changes that occur as ethane is excited in different modes. The rotational analysis shows that the B value decreases slightly in going from the $v_4=0$ to the $v_4=1$ state. The moments of inertia of ethane are easily shown to be

$$I_a=6m_H[r\sin(\mathrm{CCH})]^2 \quad (a=\text{symmetry axis}), \tag{5}$$

$$I_b=\tfrac{1}{2}m_C R^2+6m_H\{[\tfrac{1}{2}R-r\cos(\mathrm{CCH})]^2 + \tfrac{1}{2}[r\sin(\mathrm{CCH})]^2\}, \tag{6}$$

where R and r are the CC and CH bond lengths and CCH is the bond angle. We note that there is no dependence on the torsional angle γ, which is defined to be $\frac{1}{2}(\chi_1-\chi_2)$, where χ_1 and χ_2 are the CH_3 rotations with respect to an arbitrary origin. Thus changes seen in the B rotational constant when the torsional mode is excited directly reflect the changes in the CC, CH, and CCH parameters. (More correctly, the rotational constants reflect the vibrational averages of the instantaneous moments of inertia, however in considering effective *changes* a simplified interpretation in terms of structural changes can be justified.)

Physically, it is reasonable that increasing the amplitude of torsion should cause the CC and CH bonds to increase somewhat, and the CCH angle also to increase as the CH bonds "splay" back in response to the increased methyl–methyl repulsions. Each of these changes would reduce B, but it is of course not possible to distinguish their relative importance from a single measured dB. Since A depends only on the distance of the H atom from the symmetry axis, knowledge of dA would be instructive but, as discussed by Moazzen-Ahmadi *et al.*,[3] this quantity is not well determined.

We have chosen to use *ab initio* calculations to obtain some insight into the relative distortions that occur as ethane twists. Optimized geometries were determined at the Hartree–Fock SCF level for a series of torsional angles using the GAUSSIAN 92 program.[16] Table VII shows the staggered equilibrium structures that result for HF/6–311+G** and MP2/6–311+G** basis sets and it is seen that both yield results in close accord with experiment. The energy and the V_3 barrier height obtained at the simpler HF/6–331+G** level are in agreement with earlier SCF calculations by Kirtman *et al.*[18] It is interesting that inclusion of electron correlation in the second basis set did not yield a barrier closer to experiment although it did give a somewhat better CH bond length. In the following, we present trends based on the HF/6–331+G** set but similar conclusions are obtained from the more lengthy MP2 calculations.

Figure 6 shows the theoretical results displayed as *changes* from equilibrium values since these are more likely to be accurate than the absolute values of the parameters. Not surprisingly, all the parameters show a functionality similar to that usually assumed for the barrier

$$V=\tfrac{1}{2}V_3[1+\cos(6\gamma)]+\tfrac{1}{2}V_6[1-\cos(12\gamma)]. \tag{7}$$

These results predict maximum "relaxations" of +0.014 Å, −0.0011 Å, and +0.450 degrees in the CC, CH, and CCH parameters, respectively, in going from staggered to the eclipsed form. Of these, only the slight *decrease* in the

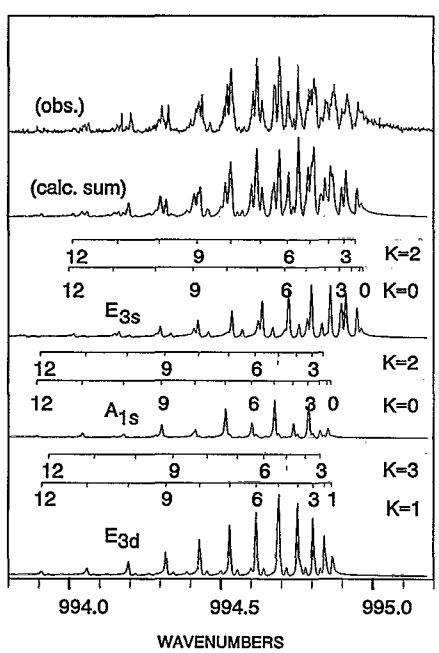

FIG. 5. Observed and simulated Q-branch spectra of E_{3s}, E_{3d}, and A_{1s} torsional components of ν_3 for C_2H_6 at 50 K.

TABLE VII. Structural parameters for C_2H_6.

	CC Å	CH Å	CCH Deg.	A cm^{-1}	B cm^{-1}	E Hartree	V_3 cm^{-1}	V_6 cm^{-1}
SCF *ab initio* results								
6–311+g**	1.5270	1.0863	111.19	2.717 55	0.669 61	−79.251 86	1071.17	9.83
MP2/6-311+g**	1.5270	1.0929	111.16	2.683 72	0.667 89	−79.609 27	1090.67	10.05
Experimental parameters[a]								
	1.5319	1.0957	111.5	2.670 54	0.663 03		1011.89	10.77
Changes on excitation from ground state								
$v_4=1$	0.003 06	−0.000 25	0.101	−0.005 00	−0.002 53[b]			
$v_4=3$	0.008 45	−0.000 65	0.275	−0.013 51	−0.006 94[c]			
$v_3=1$	0.010 09	−0.000 22	−0.118	−0.003 27[d]	−0.006 21[e]			

[a]Bond distances, angles are R_z values from Ref. 17; other parameters from Ref. 3.
[b]Changes determined by dB value from Ref. 13.
[c]Changes determined by dB value from Ref. 19.
[d]CH and CCH changes determined by dA value.
[e]CC change determined by dB value.

CH bond length is counterintuitive since both H–H repulsions and rehybridization changes with CCH angle would predict an increase. Using force constants from Ref. 19, these excursions correspond to energy lowerings of 21.4, 0.90, and 5.0 cm^{-1}, respectively, and it is clear that most (78%) of the relaxation energy comes from the extension of the CC bond as the molecule twists.

To relate these curves to the measured dB values, it is necessary to choose an averaged torsional angle for the ground state. In the $v_4=0$ level, the root mean square torsional amplitude is 5.50 degrees in the harmonic oscillator approximation, nearly identical to a value of 5.52 degrees which we calculate numerically for the torsional wave function resulting from the potential of Ref. 3. This serves then as a reference point in using the infrared dB difference of −0.002 53 cm^{-1} to deduce an effective amplitude of 11.0 degree for the $v_4=1$ level. This value is somewhat larger than the harmonic prediction of 9.5 degrees, as might be expected since this level is nearly halfway up the potential well. For the $v_4=3$ level, the experimental dB value of Henry *et al.*[20] leads to an amplitude of 18.6 degrees, again significantly higher than the harmonic oscillator value of 14.6. The vertical lines drawn in Fig. 6 thus serve as a basis for predicting the relative structural changes that occur on torsional excitation, as summarized in Table VII. Again, the most important response of the molecule to increased twisting is a small extension of the CC bond, accompanied by a slight increase in CCH angle. The same trends, but larger magnitudes, occur for higher v_4 levels.

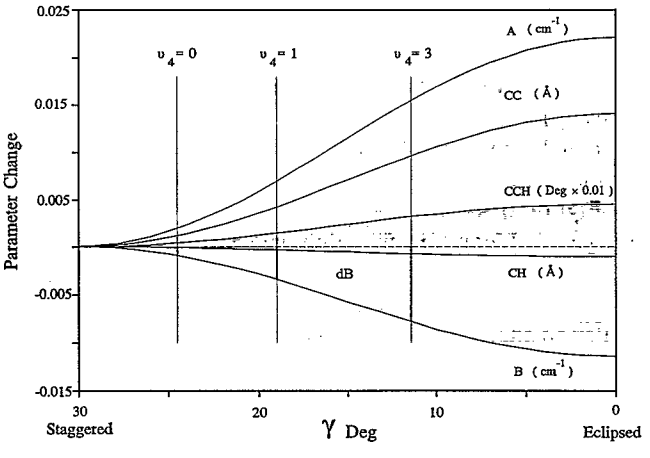

FIG. 6. *Ab initio* predictions of effect of twisting on structural parameters of C_2H_6. The vertical lines show the torsional amplitudes deduced from experimental dB values as described in the text.

B. Effect of CC excitation

The Q-branch analysis shows that the A and B rotational constants decrease slightly (−0.003 27 and −0.006 21 cm^{-1}, respectively) when the CC stretching mode is excited. The change in B is consistent with the expected longer average CC distance in the $v_3=1$ state, but the decrease in A can come only from an accompanying movement of the H atoms *away* from the symmetry axis. To explore the relative importance of these changes, *ab initio* calculations for the staggered form were done in which the CC distance was stepped and the CCH and CH parameters were varied to obtain the lowest energy. The results are shown in Fig. 7 where a clear linear variation of all the parameters with CC distance is seen.

Because of this linear relation, the effective changes in the parameters can be deduced directly from either measured dA or dB values. The value of dB predicts a CC increase of 0.010 Å, nearly the same as that from dA (0.011 Å). Since dA is a function only of H atom position [Eq. (5)] we use it to calculate a CCH bond angle decrease of 0.12 degrees and a very small CH decrease of 0.0002 Å. Both changes are consistent with the limiting case of two planar methyl radicals where the CCH "angle" would be 90 degrees and the CH distance is 0.0167 Å shorter[21] than in ethane.

We have also repeated the series of calculations for the eclipsed form and subtraction of the corresponding energies of the staggered form gives a nearly linear relation in the V_3 barrier height with CC distance. At the equilibrium position, the slope is $dV_3/dR=-3200$ cm^{-1}/Å, indicating that the effective height *decreases* by 32 cm^{-1} when the CC

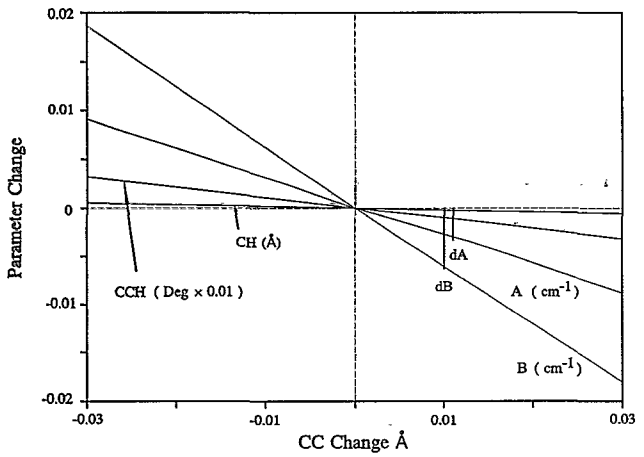

FIG. 7. *Ab initio* predictions of effect of CC stretching on structural parameters of C_2H_6. Changes predicted from the experimental dA and dB values are indicated with the bold lines.

stretch is excited by one quantum. This may be contrasted with *increases* of 99, 141, and 33 cm^{-1} when the mode excited is ν_9 (E_u rock), ν_{11} (E_g CH_3 bend), and ν_{12} (E_g rock), respectively.[9] It should be noted that the latter values are deduced from analyses of torsional splittings seen for vibrations involving these modes rather than from the simple approach used here. The higher barriers for the three E-type modes suggest that distortions from the most symmetric form makes torsion about the CC bond more difficult. In contrast, extension of the CC bond makes it somewhat easier to twist the molecule. One might predict a similar negative change in V_3, but smaller magnitude, for other A modes where the threefold symmetry is retained, such as the CH stretch and CH_3 bends.

The average of the E_{3s}, E_{3d}, A_{1s}, and A_{3d} vibrational frequencies (994.626 cm^{-1}) obtained from this work agrees well with the 994.8 cm^{-1} value obtained by Romanko *et al.*[7] from an analysis of Raman O and S branch lines. The Q-branch deconvolution procedure used in Ref. 4 in obtaining a lower value of 992.9 cm^{-1} did not take into account the torsional sublevels and should be discounted. It is gratifying that the spectral interpretation and the component frequencies deduced independently at OSU are in excellent accord with the Madrid results from the stimulated Raman spectra.[10] Since the latter are at somewhat higher resolution and are not subject to small frequency shifts due to the CARS interference effects mentioned earlier, we refer the reader to this work for a more complete discussion of the Fermi resonance interaction.

V. CONCLUSIONS

These studies show some of the potential of the CARS technique for the high resolution measurement of pure rotational and vibrational spectra. Of special aid for complex systems is the fact that the sensitivity is sufficient to obtain good spectra of samples cooled in free jet expansions. In the case of ethane, the pure rotational spectra of the ground and torsionally excited states have been combined with *ab initio* calculations to obtain insight into the structural relaxations that occur as the molecule twists. In similar fashion, bond length and bond angle changes on excitation of the CC stretch are deduced from the analysis of the complex ν_3 Q-branch structure. This transition is especially intriguing since it is a "textbook" example illustrating the interesting feature of sublevels produced by a torsional barrier and further split by Fermi resonance interactions, with transitions and nuclear spin weights that can only be understood in terms of the full double group symmetry representation.

ACKNOWLEDGMENTS

Research support by the National Science Foundation (Grant No. CHE-9014795) is gratefully acknowledged. We wish also to thank Dr. David Hassett, Dr. John Loeser, and Dr. Ian Mills for interesting discussions and helpful assistance with aspects of the torsional problem for ethane.

[1] See, for example, J. D. Kemp and K. J. Pitzer, J. Chem. Phys. **4**, 749 (1936); R. M. Pitzer, Acc. Chem. Res. **16**, 207 (1983).
[2] S. Weiss and G. E. Leroi, J. Chem. Phys. **48**, 962 (1968).
[3] N. Moazzen-Ahmadi, H. P. Gush, M. Halpern, H. Jagannath, A. Leung, and I. Ozier, J. Chem. Phys. **88**, 563 (1988).
[4] K. Van Helvoort, W. Knippers, R. Fantoni, and S. Stolte, Chem. Phys. **111**, 445 (1987).
[5] J. M. Fernandez-Sanches, A. D. Valdenebro, and S. Montero, J. Chem. Phys. **91**, 3327 (1989).
[6] B. P. Stoicheff, Can. J. Phys. **40**, 358 (1962).
[7] J. Romanko, T. Feldman, and H. Welsh, Can. J. Phys. **33**, 588 (1955).
[8] J. T. Hougen, J. Mol. Spectrosc. **82**, 92 (1980).
[9] J. Susskind, D. C. Reuter, D. E. Jennings, S. J. Daunt, W. E. Blass, and G. W. Halsey, J. Chem. Phys. **77**, 2728 (1982).
[10] D. Bermejo, J. Santos, P. Cancio, J. M. Fernandez-Sanchez, and S. Montero, J. Chem. Phys. (in press).
[11] K. W. Brown, N. H. Rich, and J. W. Nibler, J. Mol. Spectrosc. **151**, 482 (1992).
[12] A. Weber, *The Raman Effect*, Vol. 2, edited by A. Anderson (Dekker, New York, 1973).
[13] S. J. Daunt, A. K. Atakan, W. E. Blass, G. W. Halsey, D. E. Jennings, D. C. Reuter, J. Susskind, and J. W. Brault, Astrophys. J. **280**, 921 (1984).
[14] W. E. Blass, G. W. Halsey, J. Susskind, D. C. Reuter, and D. E. Jennings, J. Mol. Spectrosc. **141**, 334 (1990).
[15] A. Owyoung, G. R. Hadley, P. Esherick, R. L. Schmitt, and L. A. Rahn, Opt. Lett. **10**, 484 (1985).
[16] GAUSSIAN 92, Revision B, M. J. Frisch, G. W. Trucks, M. Head-Gordon, P. M. W. Gill, M. W. Wong, J. B. Foresman, B. G. Johnson, H. B. Schlegel, M. A. Robb, E. S. Replogle, R. Gomperts, J. L. Andres, K. Raghavachari, J. S. Binkley, C. Gonzalez, R. L. Martin, D. J. Fox, D. J. Defrees, J. Baker, J. J. P. Stewart, and J. A. Pople (Gaussian, Inc., Pittsburgh, 1992).
[17] K. Kuchitsu, J. Chem. Phys. **49**, 4456 (1968).
[18] B. Kirtman, W. E. Palke, and C. S. Ewig, J. Chem. Phys. **64**, 1883 (1976).
[19] J. L. Duncan, R. A. Kelly, B. D. Nivellini, and F. Tullini, J. Mol. Spectrosc. **98**, 87 (1983).
[20] L. Henry, A. Valentin, W. J. Lafferty, J. T. Hougen, V. Malathy Devi, P. P. Das, and K. Narahari Rao, J. Mol. Spectrosc. **100**, 260 (1983).
[21] N. E. Triggs, M. Zahedi, J. W. Nibler, P. DeBarber, and J. W. Valentini, J. Chem. Phys. **96**, 1822 (1992).